DIGITAL MODELING OF BRIDGE DRIVING-POINT ADMITTANCES FROM MEASUREMENTS ON VIOLIN-FAMILY INSTRUMENTS

Esteban Maestre
CCRMA – Stanford University
MTG – Universitat Pompeu Fabra
esteban@ccrma.stanford.edu

Gary P. Scavone
CAML/CIRMMT – McGill University
gary@music.mcgill.ca

Julius O. Smith III
CCRMA – Stanford University
jos@ccrma.stanford.edu

ABSTRACT

We present a methodology for digital modeling of D-dimensional driving-point bridge admittances from vibration measurements on instruments of the violin family. Our study, centered around the two-dimensional case for violin, viola, and cello, is based on using the modal framework to construct an admittance formulation providing physically meaningful and effective control over model parameters. In a first stage, mode frequencies and bandwidths are estimated in the frequency domain via solving a non-convex, constrained optimization problem. Then, mode amplitudes are estimated via semidefinite programming while enforcing passivity. We obtain accurate, low-order digital admittance models suited for real-time sound synthesis via physical models.

1. INTRODUCTION

String instruments, such as in the violin family, radiate sound indirectly: energy from a narrow vibrating string is transferred to a radiation-efficient body of larger surface area. To a large extent, sound radiation is produced due to the transverse velocity of the instrument body surfaces (e.g., the front or back plates), and such surface motion is transferred to the body through the force that the string exerts on the instrument's bridge. The way in which the input force at the bridge is related to the transverse velocities of the body surfaces depends on very complex mechanical interactions among the bridge itself, the sound post, the front and back plates, the air inside the body cavity, the neck, etc. Because of the importance of the bridge in mechanically coupling the strings and the body, the relation between applied force and induced velocity at the bridge has been an object of study for over forty years [1].

In the context of sound synthesis, we are interested in constructing efficient physical models of violin-family instruments. We aim to design digital filters that accurately represent the string termination as observed from the string-bridge interaction of real instruments. We model transverse string motion by means of two-dimensional digital waveguides [2] with orthogonal internal coupling.

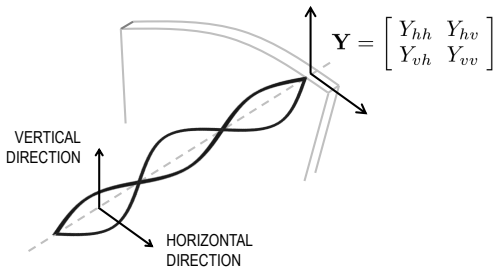

Figure 1. Two-dimensional bridge driving-point admittance.

The admittance is a physical measure used to map applied force to induced motion in a mechanical structure. In the frequency domain, the velocity vector $\mathbf{V}(\omega)$ and force vector $\mathbf{F}(\omega)$ at a position of the structure are related via the *driving-point* admittance matrix function $\mathbf{Y}(\omega)$ by $\mathbf{V}(\omega) = \mathbf{Y}(\omega)\mathbf{F}(\omega)$. In order to emulate horizontal and vertical wave reflection and transmission at the bridge, we need to construct a digital representation of matrix $\mathbf{Y}(\omega)$ in two dimensions, as represented in Figure 1, where subindexes indicate string (horizontal and vertical) polarizations, and $Y_{hv} = Y_{hv}$ (symmetric admittance). By taking measurements $\mathbf{Y}$ from real instruments, one can pose this as a system identification problem where a parametric model $\hat{\mathbf{Y}}$ is tuned so that an error measure $\varepsilon(\mathbf{Y}, \hat{\mathbf{Y}})$ is minimized.

Leaving aside approaches based on convolution with measured impulse responses, a first comprehensive work on efficient digital modeling of violin bridge admittances for sound synthesis was by Smith [3], where he proposed and evaluated several techniques for automatic design of common-denominator IIR filter parameters from admittance measurements, making real-time violin synthesis an affordable task. However, while efficiency and accuracy can be well accomplished (also when applied to other string instruments [4]), positive-realness (passivity) [2] cannot be easily guaranteed with common-denominator IIR schemes, leading to instability problems when used to build string terminations. In that regard, the modal framework [5] offers a twofold advantage: (i) admittance can be represented through a physically meaningful formulation, and (ii) positive-realness can be guaranteed.

The modal framework has been used extensively to study the mechanical properties of violins and other string instruments [1], but only recently was applied to synthesize positive-real admittances by fitting model parameters to

measurements. In a recent paper [6], Bank and Karjalainen construct a positive-real driving-point admittance model of a guitar bridge by combining all-pole modeling and the modal formulation: they first tune parameters of a common denominator IIR filter from measurement data, and use the roots of the resulting denominator as a basis for modal synthesis, so that positive-realness can be enforced. We tackle a similar problem for the case of violin-family instruments, but using the modal formulation throughout the complete fitting process.

The basic principle of the modal framework is the assumption that a vibrating structure can be modeled by a set of resonant elements satisfying the equation of motion of a damped mass-spring oscillator, each representing a natural mode of vibration of the system. Assuming linearity, the individual responses from the resonant elements (modes) to a given excitation can be summed to obtain the response of the system [7]. In theory, a mechanical structure presents infinite modes of vibration, and experimental modal analysis techniques allow to find a finite subset of (prominent) modes that best describe the vibrational properties as observed from real measurements. In general, admittance analysis via the modal framework begins from velocity measurements taken after excitation of the structure with a given force impulse function.

As introduced in [6], a useful set of structurally passive D-dimensional driving-point admittance matrices can be expressed in the digital domain as

$$\hat{\mathbf{Y}}(z) = \sum_{m=1}^{M} H_m(z)\,\mathbf{R}_m, \qquad (1)$$

where $\mathbf{R}_m$ is a $D \times D$ positive semidefinite (nonnegative definite) matrix, and each scalar modal response

$$H_m(z) = \frac{1 - z^{-2}}{(1 - p_m z^{-1})(1 - p_m^* z^{-1})}$$

is a second-order resonator determined by a pair of complex conjugate poles p_m and p_m^* [5, 6]. The numerator $1 - z^{-2}$ is the bilinear-transform image of s-plane zeros at dc and infinity, respectively, arising under the "proportional damping" assumption [5, 6]. It can be checked that $H_m(z)$ is positive real for all $|p_m| < 1$ (stable poles). In Section 3 below, we will estimate p_m in terms of the natural frequency ω_m (rad/s) and the *half-power* bandwidth B_m (Hz) of the m-th resonator, which are related to the z-domain pole p_m respectively by $\omega_m = \angle p_m / T_s$ and $B_m = \log|p_m| / \pi T_s$, where $\angle p_m$ and $|p_m|$ are the angle and radius of the pole p_m in the z-plane, and T_s is the sampling period [2].

Since the admittance model $\hat{\mathbf{Y}}(z)$ is positive real (passive) whenever the gain matrices $\mathbf{R}_m$ are positive semidefinite, the passive bridge-modeling problem can be posed as finding poles p_m and positive-semidefinite gain matrices $\mathbf{R}_m$ such than some error measure $\varepsilon(\mathbf{Y}, \hat{\mathbf{Y}})$ is minimized.

In [6], poles from an all-pole IIR fit are used as the modal basis to estimate $\mathbf{R}_m$. Once the common-denominator IIR filter has been estimated from measurement data, they find matrices $\mathbf{R}_m$ as follows: First, they independently solve three one-dimensional linear projection problems, each corresponding to an entry in the upper triangle of matrix $\mathbf{Y}$.

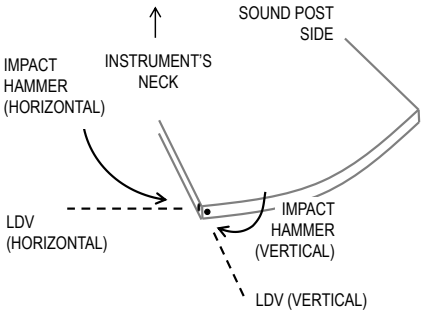

Figure 2. Illustration of the two-dimensional measurement.

This leads to three length-M modal gain vectors. Then, since simply rearranging such gain vectors as a set of M independent 2×2 symmetric gain matrices (matrices $\mathbf{R}_m$ of Equation (1)) does not enforce passivity (all of the $\mathbf{R}_m$ need to be positive semidefinite), the authors ensure passivity by computing the spectral decomposition of each $\mathbf{R}_m$, and recompose each matrix after discarding any negative eigenvalues and corresponding eigenvectors.

In this work, we deal with violin, viola, and cello bridge driving-point admittance measurements obtained from deconvolution of bridge force and velocity signals, acquired by impact excitation and motion measurement via a calibrated hammer and a commercial vibrometer (Section 2). Based on the modal formulation, we estimate modal parameters in the frequency domain via spectral peak processing and optimization of mode natural frequencies and bandwidths (Sections 3, 4, and 5). Then, we use semidefinite programming to obtain modal gain matrices by solving a matrix-form, convex problem while enforcing passivity via a non-linear, semidefinite constraint (Section 5).

2. MEASUREMENTS

We carried out zero-load bridge input admittance measurements on three decent quality instruments (violin, viola, and cello) from the Schulich School of Music at McGill University. The instruments were held in a vertical position by means of a metallic structure constructed from chemistry stands. Clamps covered by packaging foam were used to rigidly hold all three instruments from the fingerboard near the neck. While the bottom part of the body of both the violin and the viola rested firmly on a piece of packaging foam impeding their free motion during the measurements, the cello rested on its extended endpin. In order to lower the characteristic frequencies of the modes of the holding structure, sandbags were conveniently placed at different locations on the chemistry stands. Rubber bands were used to damp the strings on both sides of the bridge. Figure 3 shows a detail of th measurement setup.

Measurements of force and velocity were performed using a calibrated PCB Piezotronics 086E80 miniature impact hammer and a Polytec LDV-100 Laser Doppler Vibrometer (LDV), both connected to a National Instruments USB-4431 signal acquisition board. The location and orientation of the impact and the LDV beam are illustrated in Figure 2. Both the hammer and the LDV were carefully oriented so

Figure 3. Detail of the violin measurement setup.

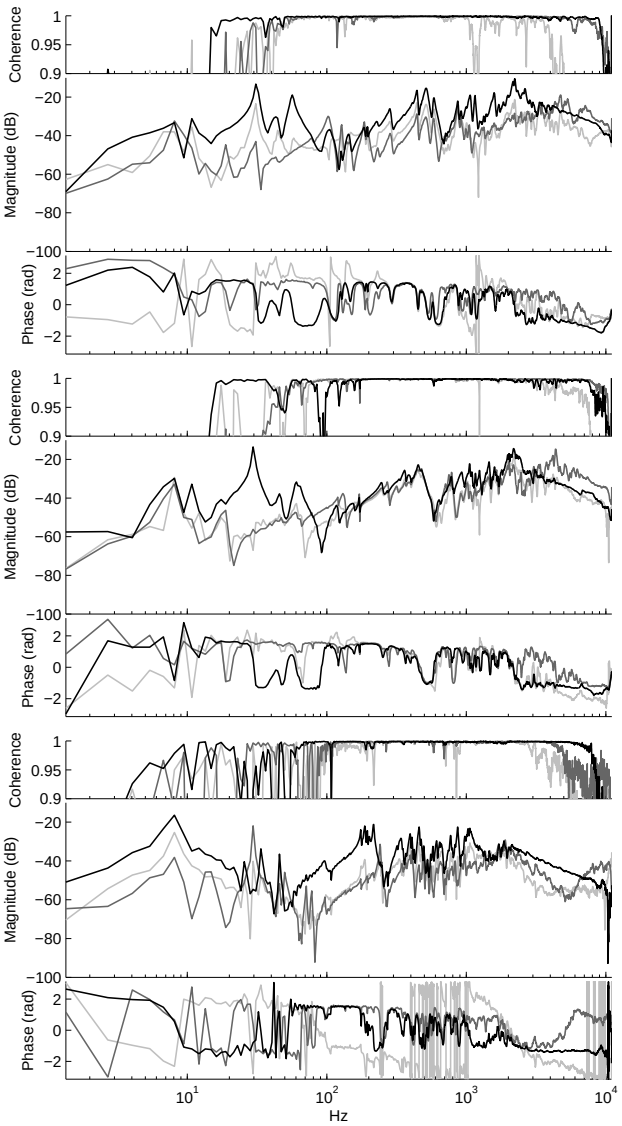

Figure 4. Admittance measurements and observed coherences. From top to bottom: coherence, magnitude, and phase of violin, viola and cello. In each plot: $Y_{hh}(f)$ (black), $Y_{vv}(f)$ (dark gray), and $Y_{hv}(f)$ (light gray) as measured at a sampling frequency of 22.05 kHz.

that impacts and measurements were as perpendicular as possible to the surface of the edge of the bridge while not interfering with each other. Time-domain signals of force and perpendicular velocity were collected, delay-compensated, and stored before computing the admittance by deconvolution. For each of the three admittance matrix entries Y_{hh}, Y_{vv}, and Y_{hv}, several measurements were collected and averaged in order to use coherence as a means for selecting the most consistent set.

Plots in Figure 4 show the frequency responses of admittance measurements Y_{hh}, Y_{vv}, and Y_{hv} performed on the violin, viola, and cello. From the responses, it is possible to make a few observations. In the region going from 100 Hz to 1 kHz approx., the characteristic modes of violin-family instruments (as extensively studied in the literature [1]) clearly appear at expected frequencies, showing moderately low overlap. Well below 100 Hz, prominent peaks appear in all measurements. Attending to the literature and previous works on normal mode analysis and identification [1], no normal modes are expected to appear at such low frequencies, leaving us with the convincing possibility that these peaks must correspond to modes of the holding structure. This was confirmed after numerous measurement trials in which the configuration of the holding structure and its position in the room were altered. Above 1 kHz, higher mode overlap leads to a broad peak (the so-called *bridge hill*), particularly prominent in the Y_{hh} measurements. It can also be observed that in the Y_{vv} responses, a second broad peak appears at a higher frequency region. Regarding phase, measurements corresponding to diagonal terms Y_{hh} and Y_{vv} present a response lying between $-\pi/2$ and $\pi/2$ (corresponding to positive-real functions), as opposed to off-diagonal terms Y_{hv}.

3. MODELING STRATEGY

Departing from admittance measurements in digital form and the M-th order modal decomposition described in Equation (1), our problem can be posed as the minimization

$$\begin{aligned} \underset{\boldsymbol{\omega},\mathbf{B},\mathbf{R}}{\text{minimize}} \quad & \varepsilon(\mathbf{Y},\hat{\mathbf{Y}}) \\ \text{subject to} \quad & \mathbf{C}, \end{aligned} \tag{2}$$

where $\boldsymbol{\omega} = \{\omega_1, \cdots, \omega_M\}$ are the modal natural frequencies, $\mathbf{B} = \{B_1, \cdots, B_M\}$ are the modal bandwidths, $\mathbf{R} = \{\mathbf{R_1}, \cdots, \mathbf{R_M}\}$ are the gain matrices, $\varepsilon(\mathbf{Y}, \hat{\mathbf{Y}})$ is the error between the measured admittance matrix $\mathbf{Y}$ and the admittance model $\hat{\mathbf{Y}}$, and $\mathbf{C}$ is a set of constraints. This problem, for which analytical solution is not available, can be solved by means of gradient descent methods that make use of local (quadratic) approximations of the error function $\varepsilon(\mathbf{Y}, \hat{\mathbf{Y}})$. Given the way our fitting problem is posed, five main issues need to be taken into consideration:

– **Design parameters**. From observation of each diagonal entry Y_{hh} and Y_{vv} of the measured admittance matrices (see Section 2), and by contrasting with relevant literature on modal analysis of violin family instruments [1], we make two assumptions. First, at low frequencies (approximately between 100 Hz and 1 kHz) modes of interest present relatively low overlap and can be identified and modeled individually. Second, at higher frequencies (above 1 kHz) high mode overlap leads to a broad peak (bridge hill) that can modeled by a single, highly-damped resonance. This leaves us with three design parameters: frequencies ω_{min} and ω_{max}, and number of low-frequency modes M. Between frequencies ω_{min} and ω_{max}, M modes are identified and modeled individually, while above ω_{max} the bridge hill is modeled by a single mode. When studying the two-dimensional case, we found that using two high-frequency modes provides a better basis for modeling the bridge hill (see Section 2 and Section 5.1).

– **Initial estimation**. Because the minimization problem, Equation (2) is not convex, it is very important to choose a starting point that is close enough to the global minimum. Therefore, it is crucial to carry out an initial estimation of mode parameters prior to optimization. The method, to be described in Section 4.1, is based on peak (resonance) picking from the magnitude spectrum, and a graphical estimation of each mode frequency and bandwidth.

– **Constraint definition**. Defining constraints on the parameters of the problem is motivated by two reasons: feasibility and convergence. First, a number of feasibility constraints are needed to obtain a realizable solution. Second, in order to ensure that the optimization algorithm will not jump into regions of the parameter space where it can get stuck in local minima, additional constraints need to be defined so that candidate solutions stay within the region of convergence.

– **Error computation**. Since there is no analytical expression for the gradient of this error minimization, it needs to be estimated from computing the error in different directions around a point in the parameter space. Therefore, we need to choose a convenient method for computing $\varepsilon(\mathbf{Y}, \hat{\mathbf{Y}})$ at any point in the parameter space.

– **Estimation of gains**. Once the M modal frequencies and bandwidths are optimized, it is necessary to perform an estimation of matrices $\mathbf{R}$ of Equation (2) to complete the model of Equation (1).

4. ONE-DIMENSIONAL MODELING

The one-dimensional procedure presented here can be used both for Y_{hh} and Y_{vv}. First, once design parameters M, f_{min}, and f_{max} have been set, individual mode resonances are identified from the magnitude spectrum through a peak picking iterative procedure. Then, an initial estimation of mode parameters (frequencies and bandwidths) is obtained via the half-power method. In a final step, mode parameters are tuned via numerical optimization.

4.1 Initial estimation

4.1.1 Peak selection

Peak selection in the low-frequency region is carried out through an automatic procedure that iteratively rates and sorts spectral peaks by attending to a salience descriptor. The high-frequency bridge hill resonance center frequency is selected via smoothing the magnitude spectrum.

4.1.2 Estimation of frequencies and bandwidths

For estimating modal frequencies, three magnitude samples (respectively corresponding to the corresponding maximum and its adjacent samples) are used to perform parabolic interpolation. For estimating bandwidths, the *half-power* rule [2] is applied using a linear approximation.

4.2 Error computation

For optimization routines to successfully approximate error derivatives, it is necessary to supply a procedure to evaluate the error function as a function of the model parameters, namely a vector $\mathbf{x}$. In our case, parameters are (see Equation 2) mode frequencies $\boldsymbol{\omega}$ and bandwidths $\mathbf{B}$. Thus $\mathbf{x}$ is constructed by concatenating elements in sets $\boldsymbol{\omega}$ and $\mathbf{B}$, leading to $\mathbf{x} = [\boldsymbol{\omega}\ \mathbf{B}]^T$. We work with frequency-domain representations of the admittance measurement Y and admittance model $\hat{Y}$. At the k-th iteration, parameter vector is $\mathbf{x}|_k$, and evaluating $\varepsilon(Y, \hat{Y}|_k)$ implies: (i) retrieving mode frequencies and bandwidths from $\mathbf{x}|_k$, (ii) estimating gains as outlined in Section 4.4, (iii) constructing a synthetic admittance $\hat{Y}|_k$ with computed gains, and (iv) computing error $\varepsilon(Y, \hat{Y}|_k)$.

Let vector $\mathbf{y} = [y_1, \ldots, y_n, \ldots, y_N]^T$ contain N samples of $Y(\omega)$, taken in $0 \leq \omega < \pi$. Analogously, let $\hat{\mathbf{y}}|_k = [\hat{y}_1|_k, \ldots, \hat{y}_n|_k, \ldots, \hat{y}_N|_k]^T$ contain N samples of $\hat{Y}(\omega)|_k$, constructed from parameter vector $\mathbf{x}|_k$. We compute the error $\varepsilon(Y, \hat{Y}|_k)$ as

$$\varepsilon(Y, \hat{Y}|_k) = \sum_{n=1}^{N} \Big| \log \frac{|y_n|}{|\hat{y}_n|_k|} \Big|, \tag{3}$$

which can be interpreted as subtracting magnitudes when expressed in the logarithmic scale.

4.3 Constraint definition

Apart from providing a reliable initial point $\mathbf{x}|_0$ (see Section 4.1), we need to define a set of constraints to be respected during the search:

– **Mode sequence order**. A first important constraint to be respected during the search is the sequence order of modes (in ascending characteristic frequency) as they were initially estimated (see Section 4.1).

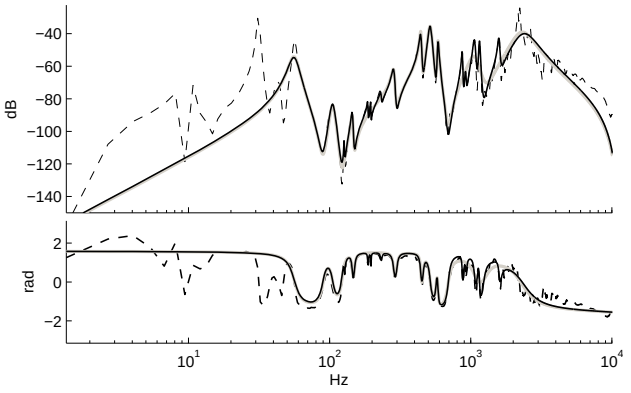

Figure 5. Synthetic admittance $\hat{Y}_{hh}$ modeling example. Magnitude (top) and phase (bottom). Dashed curves: admittance measurement; solid gray curves: $M = 7$, $f_{\text{min}} = 50$ Hz, $f_{\text{max}} = 1300$ Hz; solid black curves: $M = 15$, $f_{\text{min}} = 50$ Hz, $f_{\text{max}} = 1700$ Hz.

– **Low-frequency region**. All of the M low-frequency modes must lie in the frequency region prescribed by design parameters ω_{min} and ω_{max}.
– **Bridge hill frequency region**. Analogous to the previous constraint, the characteristic frequency of the bridge hill resonance must be within the limits set by additional design parameters ω^b_{min} and ω^b_{max}.
– **Positive bandwidth**. Bandwidths must be positive.
– **Distance from initial estimation**. Assuming the initial estimation $\mathbf{x}|_0$ is close enough to the final solution, one can bound the search space around $\mathbf{x}|_0$.

All constraints are linear in parameters $\mathbf{x}$, and Equation (2) can be efficiently solved via sequential quadratic programming by means of Matlab's Optimization Toolbox [8].

4.4 Estimation of gains

At any k-th iteration of the optimization procedure, modal gains can be obtained via solving a constrained linear projection problem. By evaluating the individual frequency responses of the $M + 1$ resonators as constructed from parameters in vector $\mathbf{x}|_k$, modal gains are found via solving the one-dimensional version of Equation (1) in the frequency domain while imposing a nonnegative constratin on the gain vector. Results for a violin admittance Y_{hh} are shown in Figure 5.

5. TWO-DIMENSIONAL MODELING

The procedure for the two-dimensional case is based on the fitting procedure for the one-dimensional case. A main assumption is made: the modes of the full system $\mathbf{Y}$ can be estimated by only attending to diagonal measurements Y_{hh} and Y_{vv}. First, diagonal entries Y_{hh} and Y_{vv} of measurement matrix $\mathbf{Y}$ are used separately to obtain two sets of modal frequencies and bandwidths (Section 4). In a second step, the two sets of modes are merged into a common mode structure, which will be used as the basis for the model $\hat{\mathbf{Y}}$. After merging, mode parameters are re-optimized by simultaneously minimizing an error between (diagonal) measurements Y_{hh} and Y_{vv}, and their respective model counterparts $\hat{Y}_{hh}$ and $\hat{Y}_{vv}$, the latter two constructed from the common mode structure under optimization. Finally, we use semidefinite programming to estimate gain matrices $\mathbf{R}$ for the full matrix model $\hat{\mathbf{Y}}$ by using all three measurements Y_{hh}, Y_{vv}, and Y_{hv}.

5.1 Initial estimation

Providing an initial estimation of mode frequencies and bandwidths consists of two main steps: independent tuning of a one-dimensional model for each entry in the diagonal of matrix $\mathbf{Y}$, and merging of mode estimations.

5.1.1 Diagonal entries

First, by means of the procedure outlined in Section 4, we carry out two one-dimensional fittings respectively corresponding to self-admittance (diagonal) measurements Y_{hh} and Y_{vv}. Design parameters are shared by both cases, except for the fact that two broad resonances are used for the high frequency region (see Section 2), meaning that two regions $(\omega^b_{hh,\text{min}}, \omega^b_{hh,\text{max}})$ and $(\omega^b_{vv,\text{min}}, \omega^b_{vv,\text{max}})$ are defined after observation of measurements.

5.1.2 Mode merging

Since many of the modes of the system get excited both in the horizontal and vertical directions (see Figure 4), the same mode may be estimated from both measurements. Joining the two sets of $M + 1$ modes independently obtained from the two one-dimensional fits leads to a set of $2(M + 1)$ mode candidates, from which pairs of numerically close mode estimations (i.e., corresponding to the same mode of the system) may appear. We merge the $2M$ mode estimations in $(\omega_{\text{min}}, \omega_{\text{min}})$ into a set of M' modes (with $M' \leq 2M$). First, we perform clustering on mode frequencies. Then, from each of the M' clusters, we keep the mode estimation presenting a natural frequency that is closest to the cluster centroid. From now on, the total number of modes, including the two bridge hill modes, will be referred to as M.

5.2 Error computation

Because optimization is carried out from measurements Y_{hh} and Y_{vv} simultaneously, we compute the diagonal modeling error ε' at iteration k as the sum of one-dimensional modeling errors when obtained through the common set of parameters (frequencies and bandwidths) $\mathbf{x}|_k$.

5.3 Constraint definition

Once initial mode estimates have been merged, constraints are defined analogously to the one-dimensional case. The only remarkable difference is the use of two broad resonances to represent the bridge hill.

5.4 Estimation of gains

We perform gain estimation by working with a frequency-domain expression of Equation (1) as described next. From a two-dimensional admittance measurement (symmetric) matrix $\mathbf{Y}$, let $\mathbf{y}_{hh}$, $\mathbf{y}_{hv}$, and $\mathbf{y}_{vv}$ be complex-valued column

vectors each containing N frequency-domain samples of its corresponding entry in $\mathbf{Y}$, leading to a $2N \times 2$ matrix of the form

$$\mathbf{Y} = \begin{bmatrix} \mathbf{y}_{hh} & \mathbf{y}_{hv} \\ \mathbf{y}_{hv} & \mathbf{y}_{vv} \end{bmatrix}. \tag{4}$$

Now, we proceed with rewriting the right-side of Equation (1) in matrix form as constructed from linear combinations of frequency-domain samples of the individual modal responses $H_m(\omega)$. First, we define a $N \times M$ matrix H as

$$\mathsf{H} = [\mathbf{h}_1, \dots \mathbf{h}_m \dots \mathbf{h}_M], \tag{5}$$

where each $\mathbf{h}_m$ is a complex column vector containing N samples of $H_m(\omega)$. With matrix H, we construct a $2N \times 2M$ block-diagonal matrix B defined as

$$\mathsf{B} = \begin{bmatrix} \mathsf{H} & 0 \\ 0 & \mathsf{H} \end{bmatrix}, \tag{6}$$

which can be interpreted as a two-dimensional modal basis. The next step is to set up a $2M \times 2M$ block-symmetric matrix R as

$$\mathsf{R} = \begin{bmatrix} \mathsf{R}_{hh} & \mathsf{R}_{hv} \\ \mathsf{R}_{hv} & \mathsf{R}_{vv} \end{bmatrix}, \tag{7}$$

where R_{hh}, R_{hv}, and R_{vv} are $M \times M$ diagonal, real matrices. In the m-th entry of the diagonal of matrix R_{hh} appears the gain from entry $(1,1)$ of the individual gain matrix $\mathbf{R}_m$ in Equation (1). Analogously, matrix R_{hv} will contain gains from the M entries $(1,2)$, and R_{vv} from entries $(2,2)$. Now, with modal basis B and gain matrix R, it is possible to write an expression for model $\hat{\mathbf{Y}}$ as

$$\hat{\mathbf{Y}} = \mathsf{BRS}, \tag{8}$$

where S is a $2M \times 2$ matrix of ones which acts as the summation of Equation (1). It is important to note that $\mathsf{R} \succeq 0 \Leftrightarrow \mathbf{R}_m \succeq 0 \ \forall m \in \{1, \dots, M\}$, implying that the model $\hat{\mathbf{Y}}$ will be passive if matrix R is positive semidefinite. Now we are ready to express the modal gain estimation problem as an error minimization problem that includes a positive semidefinite constraint on matrix R. If expressing the model approximation error $\varepsilon(\mathbf{Y}, \hat{\mathbf{Y}})$ as

$$\varepsilon(\mathbf{Y}, \hat{\mathbf{Y}}) = \|(\hat{\mathbf{Y}} - \mathbf{Y})\| = \|(\mathsf{BRS} - \mathbf{Y})\|, \tag{9}$$

where $\|\cdot\|$ represents a suitable matrix norm, the problem can be written as

$$\begin{aligned} \underset{\mathsf{R}}{\text{minimize}} \quad & \|(\mathsf{BRS} - \mathbf{Y})\| \\ \text{subject to} \quad & \mathsf{R} \succeq 0, \end{aligned} \tag{10}$$

which is a matrix norm minimization problem with a positive semidefinite constraint. This convex problem can be solved via semidefinite programming by means of CVX, a package for specifying and solving convex programs [9].

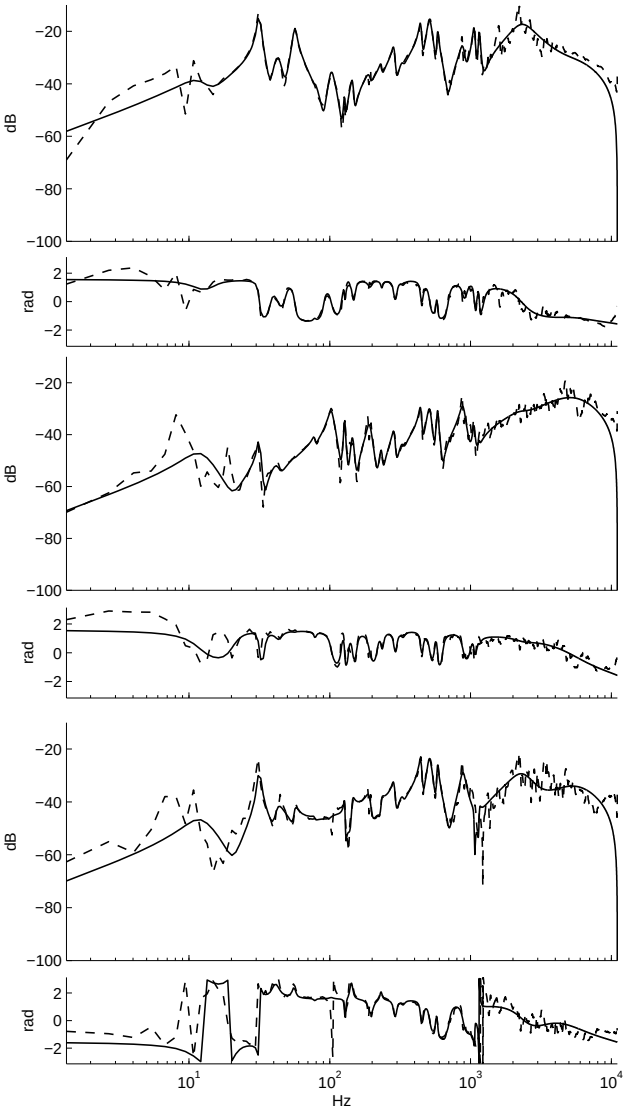

Figure 6. Violin synthetic admittance matrix $\hat{\mathbf{Y}}$ modeling example. Top to bottom, magnitude and phase plots of $\hat{Y}_{hh}(f)$, $\hat{Y}_{vv}(f)$, and $\hat{Y}_{hv}(f)$. $M = 18$, $f_{\text{min}} = 8$ Hz, $f_{\text{max}} = 1300$ Hz.

6. RESULTS AND DISCUSSION

Modeling examples for violin, viola, and cello are respectively shown in Figure 6, 7, and 8. In all three cases, with respective model orders between $M = 18$ and $M = 27$, high accuracy (including phase matching) can be observed between 100 Hz and 6 KHz, where measurement coherence was acceptable. In particular for the cello, the interaction between modes of the measurement apparatus and lower-frequency modes of the instrument made measuring and modeling a more difficult task. In general, both accuracy and convergence times are improved if carrying out the estimation on a warped frequency axis [3, 10]. Moreover, truncation of spectral domain samples above 6 kHz was needed in order to avoid artifacts caused by measurement limitations.

It is very important to include the lower frequency region (i.e., between 5 Hz and 100 Hz) in the fitting process

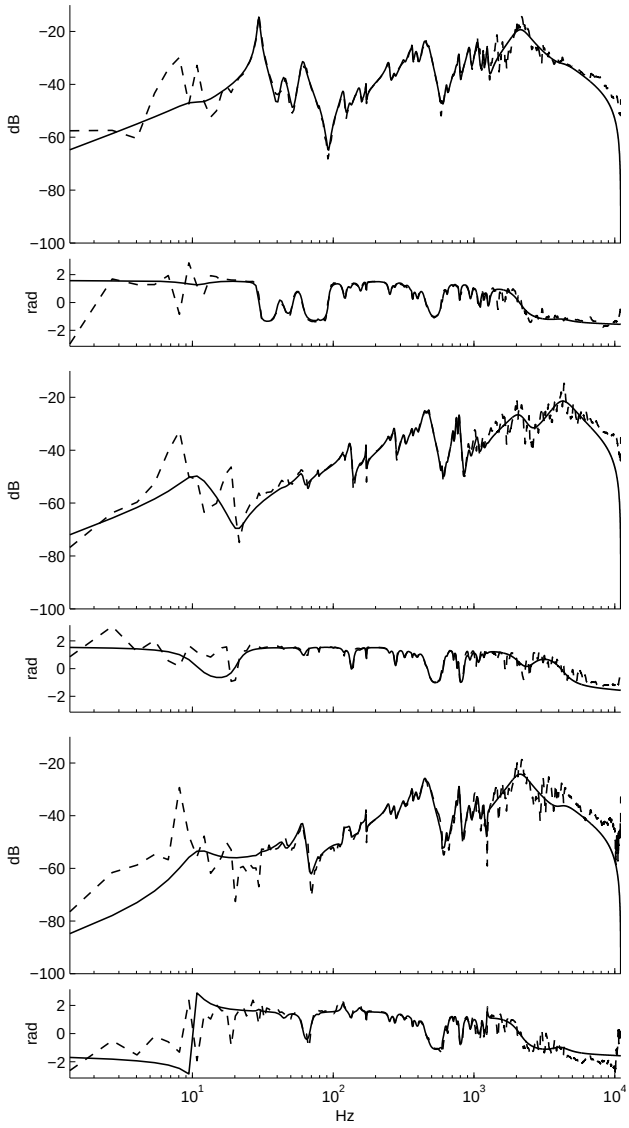

Figure 7. Viola synthetic admittance matrix $\hat{\mathbf{Y}}$ modeling example. Top to bottom, magnitude and phase plots of $\hat{Y}_{hh}(f)$, $\hat{Y}_{vv}(f)$, and $\hat{Y}_{hv}(f)$. $M = 22$, $f_{\text{min}} = 8$ Hz, $f_{\text{max}} = 1300$ Hz.

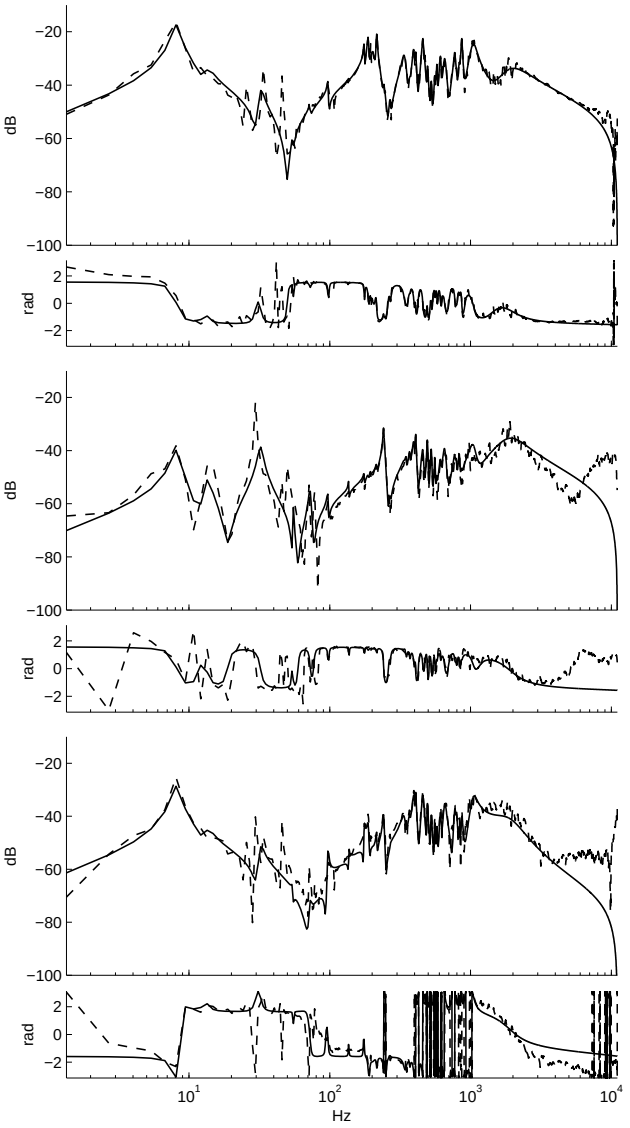

Figure 8. Cello synthetic admittance matrix $\hat{\mathbf{Y}}$ modeling example. Top to bottom, magnitude and phase plots of $\hat{Y}_{hh}(f)$, $\hat{Y}_{vv}(f)$, and $\hat{Y}_{hv}(f)$. $M = 27$, $f_{\text{min}} = 8$ Hz, $f_{\text{max}} = 900$ Hz.

by setting design parameter ω_{min} close to dc. This allows the modes of the measurement apparatus (prominent peaks below 100 Hz) to also be modeled, leading to a more consistent overall estimation that accounts for the interaction of such modes with the *real* modes of the instrument. Once the estimation is finished, those modes and their respective gain matrices can be discarded from Equation (1).

Regarding implementation, an elegant re-formulation of second-order sections proposed in [11] and later applied in [6] allows to maintain the parallel structure, leading to a straightforward realization as a reflectance. Our results from applying such re-formulation have been used to construct lumped terminations where four two-dimensional digital waveguides are coupled without the need for parallel adaptors (as in wave digital filters—see [6]). Example sounds, including one-pole filters to simulate string losses, are available online [1] . The application of these models to bowed-string simulation with two-dimensional transverse string motion is imminent.

A potential improvement to the fitting method goes around embedding the semidefinite programming step as part of an outer loop in which mode parameters are estimated, although it would imply a higher computational cost. By increasing the model order and redefining design parameters it would be possible to represent the bridge hill region more accurately; yet, a perceptual evaluation might be needed to confirm improvements. Further tests might encourage the construction of statistical admittance models, where modal frequencies, bandwidths, and amplitudes follow empirically inferred distributions. An extension of the framework to include radiation measurements is currently under study.

[1] `http://ccrma.stanford.edu/~esteban/adm/smac13`

Acknowledgments

This work was partially funded by the Catalan Gov. through a Beatriu de Pinós Fellowship. Thanks go to Argyris Zymnis and Jonathan S. Abel for inspiring discussions.

7. REFERENCES

[1] T. Rossing, *The Science of String Instruments*. Springer New York, 2010.

[2] J. O. Smith, *Physical Audio Signal Processing, December 2008 Edition*. http://ccrma.stanford.edu/~jos/pasp/, accessed 2012, online book.

[3] ——, "Techniques for digital filter design and system identification with application to the violin," Ph.D. dissertation, Stanford University, 1983.

[4] M. Karjalainen and J. O. Smith, "Body modeling techniques for string instrument synthesis," in *Proc. of the International Computer Music Conference*, 1996.

[5] K. D. Marshall, "Modal analysis of a violin," *Journal of the Acoustical Society of America*, vol. 77:2, pp. 695–709, 1985.

[6] B. Bank and M. Karjalainen, "Passive admittance matrix modeling for guitar synthesis," in *Proc. of the 13th International Conference on Digital Audio Effects*, 2010.

[7] J. M. Adrien, "The missing link: Modal synthesis," in *Representations of Musical Signals*, G. D. Poli, A. Piccialli, and C. Roads, Eds. MIT Press, 1991, pp. 269–267.

[8] MATLAB, *version 7.10.0 (R2010a)*. Natick, Massachusetts: The MathWorks Inc., 2010.

[9] M. Grant and S. Boyd, "CVX: Matlab software for disciplined convex programming, version 1.21," http://cvxr.com/cvx/, Apr. 2011.

[10] A. Härmä, M. Karjalainen, L. Savioja, V. Välimäki, U. K. Laine, and J. Huopaniemi, "Frequency-warped signal processing for audio applications," *Journal of the Audio Engineering Society*, vol. 48(11), pp. 1011–1031, 2000.

[11] M. Karjalainen, "Efficient realization of wave digital components for physical modeling and sound synthesis," *IEEE Trans. Audio, Speech, and Lang. Process.*, vol. 16:5, pp. 947–956, 2008.